The constrained optimisation of small linear arrays of heaving point absorbers. Part I: The influence of spacing

Justin P.L. McGuinness, Gareth Thomas

PII: S2214-1669(17)30060-7
DOI: http://dx.doi.org/10.1016/j.ijome.2017.07.005
Reference: IJOME 161

To appear in:

Received Date: 30 December 2016
Accepted Date: 17 July 2017

Please cite this article as: J.P.L. McGuinness, G. Thomas, The constrained optimisation of small linear arrays of heaving point absorbers. Part I: The influence of spacing, (2017), doi: http://dx.doi.org/10.1016/j.ijome.2017.07.005

The Constrained Optimisation of Small Linear Arrays of Heaving Point Absorbers. Part I: The Influence of Spacing

Justin P.L. McGuinness[a,b,*], Gareth Thomas[a]

[a] *Department of Applied Mathematics, University College Cork, Ireland*
[b] *Department of Mathematics, Cork Institute of Technology, Ireland*

Abstract

This paper describes the optimisation of small arrays of Wave Energy Converters (WECs) of point absorber type. The WECs are spherical in shape and operate in heave alone and a linear array of five devices is considered. Previous work is extended by considering the constrained performance of the array members, where an upper limit on WEC displacements is enforced. Two optimisations are performed. In each case, the objective function is defined as the mean of the averaged interaction factor over the non-dimensional length of the array. The first considers the array layout fixed at a geometry previously identified as optimal in an unconstrained regime and optimises the displacements of the WECs subject to constraints. The second allows both the WEC positions and displacements to vary as optimisation variables. It is shown that the optimal layout of the constrained arrays is different from the unconstrained case. Applying constrained motions results in optimal

*Corresponding author
Email addresses: j.mcguinness@umail.ucc.ie (Justin P.L. McGuinness), g.thomas@ucc.ie (Gareth Thomas)

layouts that are more separated, with less grouping of WECs and this will have practical considerations. The effect of the constraints varies depending on the incident wave angle. In some cases, performance is reduced drastically and stability of performance is improved, while in other cases there is a degradation of performance. Thus, a trade-off between performance and stability of performance is seen when displacement constraints are applied.
Keywords: Wave-Power, Arrays, Constrained Optimisation, Interaction, Point Absorber

1. Introduction

The fundamental modelling of arrays of wave power devices of point absorber type was presented independently in [1] and [2]. The point absorber approximation assumes that the ratio of device size to incident wavelength is small enough for the scattered wave field of the device to be neglected. This allows a simplification of the calculations, particularly those relating to WEC arrays. Subsequent papers have applied this theory to assess arrays of differing configurations or array properties, e.g. [3, 4, 5, 6, 7, 8].

In [1],[2] and [3], the devices were assumed to be equally spaced and the concept of positive and negative interference within the array was established. The concept of unequal spacing in a linear array was first considered in [4] and it was shown that unequally spaced arrays performed better in some cases in comparison to equally spaced arrays. However, only a very specific case of unequal spacing was considered. The accuracy of the point absorber approximation is discussed in [5], where it is shown that the approximation gives agreement with the exact multiple scattering method for

a non-dimensional device radius of $ka < 0.8$. The extension to arbitrary array arrangements, without any stipulated geometry or symmetry is considered in [6], [7] and [8]. In [6] and [7], the point absorber approximation is applied and the interaction factor is numerically maximised with respect to WEC positions for both constrained and unconstrained WEC motions. A full interaction regime is implemented in [8] and the array performance is maximised using a genetic algorithm for both regular and irregular waves.

A major common finding of the of the previous array optimisation studies (e.g. [3], [6], [7] and [8]) is that the optimal array arrangements were often found to be only slightly different to those corresponding to very poorly performing arrays. In many cases, either the best and worst array layouts were surprisingly close or the optimal array had a sharp peak in performance surrounded by large troughs. This means that a small change in the non-dimensional parameters of such arrays, either by a physical mis-alignment or a change in sea conditions (incident wavelength or wave angle), can have a potentially disastrous impact on array performance.

This issue was addressed in [9] and [10], which considered the optimisation of linear and circular arrays of five to seven WECs, where the mean of the interaction factor was maximised, rather than the interaction factor itself. In these works, the mean was taken over a non-dimensional lenght/radius measure, which resulted in arrays that were stable to changes in non-dimensional separation parameters. However, in some cases, these optimal arrays were still quite sensitive to changes in incident wave angle. One important issue is whether high performance or stability (reliability) of performance is more desirable. Ideally, both would be achieved by an optimal array, however

this may not be possible, particularly with the application of WEC motion constraints.

A main concern when considering array performance is the motions of the individual devices associated with optimal performance. A hydrodynamically optimised array is typically accompanied by large amplitude device motions; this is highlighted in [10]. The large motion of WECs creates engineering difficulties with the control, maintenance and power take-off of the devices. In addition, linear wave theory assumes that all device motions are at most of the same order of the wave amplitude, and violation of this requirement invalidates the underlying assumptions; this is considered in [3], [6], [9] and [10], where the optimal arrays were predicted to exhibit large device motions. Device motion constraints were investigated in [3] and [6], where it was found that, in some cases, these constraints severely limited array performance.

The main aim of this paper is the constrained optimisation of WEC arrays such that the resulting optimal array is stable to changes in array parameters. Having an array that performs well in certain conditions but that is also highly sensitive to changes in wavelength or wave angle is not ideal. Wave conditions in the open ocean can change slightly and ideally a WEC array should maintain optimal or at least near-optimal performance in the case of any such changes. Previous research of the nature is extended by considering constrained performance of the WECs, where the WEC motions are limited to two or three times the incident wave amplitude, as in [3] and [6]. The effect of these constraints are firstly analysed with respect to layouts previously optimised without constraints. The layouts are then re-optimised within the constrained regime and the resulting layouts compared.

The work presented herein is conducted within the regime of validity of the point absorber approximation ($ka < 0.8$) as identified in [5], and the non-dimensional radius of the WECs is fixed at $ka = 0.4$. An external model is required in this methodology to determine the device motions and for the chosen device geometry, which is spherical in this case, the motions can be determined using the approach of [11], for a fixed non-dimensional radius of the WECs.

This research is motivated by the possibility that unequally spaced linear arrays may perform better that their equally spaced analogs. The work presented in [9] and [10] was similarly motivated, where linear and circular array geometries were enforced and the mean array performance was maximised with respect to the non-dimensional WEC separations. The mean performance was defined over a range of non-dimensional array length or radius.

Section 2 outlines the mathematical theory behind this research, including the definition of the averaged interaction factor for constrained motions and the optimisation method. The results of the optimisation are presented in section 3. The constrained performance of previously identified unconstrained optimal array layouts is assessed in section 3.1. In section 3.2, the array layout is not prescribed and an optimisation over both the WEC motions and positions is performed with respect to the mean of the averaged interaction factor. Finally, a discussion of the results is given in section 4 along with some conclusions thereof.

2. Mathematical Formulation

2.1. Power Absorption Theory

Consider a linear array of physical length L with N semi-submerged spheres, considered to be point absorbers and which operate in heave alone. It is assumed that linear wave theory is applicable and that regular long-crested waves of amplitude A, frequency ω, wavenumber k and angle β are incident on the array in water of infinite depth, where β is measured in an anticlockwise direction from the positive x-axis.

A detailed description of the background theory is available in [9] and [10], where array power absorption theory and the point absorber approximation are outlined. In this work, constrained motions are considered and the full power absorption equation is employed without the assumption of optimal motions. As shown in [1], the mean power absorbed by the array is

$$P_{abs} = \frac{1}{8}\mathbf{X}^{\dagger}\mathbb{B}^{-1}\mathbf{X} - \frac{1}{2}\left(\mathbf{U} - \frac{1}{2}\mathbb{B}^{-1}\mathbf{X}\right)^{\dagger}\mathbb{B}\left(\mathbf{U} - \frac{1}{2}\mathbb{B}^{-1}\mathbf{X}\right), \tag{1}$$

where $\mathbf{X}$ and $\mathbf{U}$ are complex time-independent column vectors of the exciting forces and velocities of the devices respectively, $\mathbb{B}$ is the radiation damping matrix and † denotes complex conjugate transpose. In this notation, the exciting force and velocity of body m are given by $\mathrm{Re}[X_m e^{-i\omega t}]$ and $\mathrm{Re}[U_m e^{-i\omega t}]$. In order to relate the body displacements to the mean power absorption of the array, the velocities are replaced by

$$\mathbf{U} = -i\omega A\mathbf{D}, \tag{2}$$

where $\mathbf{D}$ is a complex time-independent column vector containing the body displacements non-dimensionalised with respect to the incident wave amplitude. The expression (1) is not optimal and holds under general conditions.

In order to assess the array performance in the constrained case, the averaged interaction factor is utilised and defined as

$$\overline{q} = \frac{\text{Power absorbed by array subject to constraints}}{N \times \text{Maximum power absorbed by isolated WEC}}. \tag{3}$$

This quantity will usually not achieve a value of unity, unless the constraints applied do not restrict the optimal motions of the WECs. It is also possible for the constrained power absorbed by the array to become negative, in which case the forced displacements cause the array to inject power into the waves, thereby creating waves rather than absorbing them. Assuming the point absorber approximation to be applicable allows the averaged interaction factor to be written, via [11], as

$$\overline{q} = \frac{4\pi(ka)^2}{N}\left(-\mathrm{Re}\left[(\mathcal{D}+i\mathcal{C})\mathbf{D}^\dagger\boldsymbol{\ell}\right] - \pi(ka)^2(\mathcal{C}^2+\mathcal{D}^2)\mathbf{D}^\dagger\mathbb{J}\mathbf{D}\right), \tag{4}$$

where a is the WEC radius, $\mathcal{C}$ and $\mathcal{D}$ are the Havelock coefficients, $\boldsymbol{\ell}$ is a column vector with components $\{\ell_m = e^{ikd_m\cos(\beta-\alpha_m)}; m = 1,\ldots,N\}$ and $\mathbb{J}$ is an $N\times N$ matrix with elements $\mathbb{J}_{mn} = J_0\left(kd_{mn}\right)$, where $J_0(x)$ is the zeroth order Bessel function of first kind.

In this notation, the position of the m^{th} device is given by the cylindrical polar coordinates $(r,\theta,z) = (d_m,\alpha_m,0)$ and d_{mn} is the distance between the m^{th} and n^{th} devices. One device is fixed at the origin, without loss of generality. As this work concerns linear arrays, all the α_m's are set to zero. In addition, as consecutive device separations are often employed, the convenient notation $s_m = d_{m(m+1)}$ is introduced.

2.2. Optimisation Process

As in [10], the aim of the hydrodynamic optimisation is to expressly seek array layouts that are stable to changes in non-dimensional parameters as-

sociated with device spacing and incident wavelength. In this paper, the constrained performance of the arrays is examined, where the displacement amplitudes of the WECs are limited to an upper value during the optimisation.

The same re-parameterisation of the separations presented in [10] is utilised here, namely

$$ks_j = n_j \; kL, \tag{5}$$

where $n_j \in (0, 1)$ is a real parameter that represents the relative separation between devices with respect to the total length. Consistency requires that

$$\sum_{j=1}^{N-1} n_j = 1, \tag{6}$$

which removes one separation variable. Furthermore, relative to [10] there are now an extra N complex displacement variables D_j. In order to formulate the objective function explicitly in terms of real variables, the non-dimensional complex displacements are written as

$$D_j = \delta_j e^{i\psi_j}, \tag{7}$$

where δ_j and ψ_j are the displacement amplitude and phase of the j^{th} WEC respectively.

Using this formulation, the objective function becomes

$$\overline{I}(\mathbf{n}, \boldsymbol{\delta}, \boldsymbol{\psi}; \beta_0) = \frac{1}{kL_u - kL_l} \int_{kL_l}^{kL_u} \overline{q}(\mathbf{n}, \boldsymbol{\delta}, \boldsymbol{\psi}, kL; \beta_0) \; d[kL], \tag{8}$$

where $\boldsymbol{\delta}$ and $\boldsymbol{\psi}$ are N-component vectors containing the motion amplitudes and phases of each device respectively, $\mathbf{n}$ is an $(N-2)$-component vector

containing the separation variables, $kL \in [kL_l, kL_u]$ is the integration variable describing the range of non-dimensional length considered and β_0 is a fixed prescribed incident wave angle. The notation $\overline{I}$ is to indicate that the mean is defined with respect to $\overline{q}$ and thus considers constrained WEC motions, which is distinct from the unconstrained optimisation in [10]. The objective function contains a total of $3N - 2$ and will be maximised using a similar procedure to that in [10], with appropriate constraints placed on the variables.

The non-dimensional parameter kL can be considered in two ways; for a fixed wavelength λ it represents a change in physical array length L, while for a fixed array length it represents a change in incident wavelength. The range of optimisation over kL is chosen to be $[kL_l, kL_u] = [5, 15]$ in this paper. These values are chosen arbitrarily but are intended to represent a typical case. The aim is to represent a target (or mean) value of $kL = 10$, with the range chosen to allow for variation around this target value. Typical ocean wavelengths are approximately 200m, in which case the target value of $kL = 10$ corresponds to an array length of approximately 320m. Considering a fixed array length of 320m, the lower bound $kL_l = 5$ corresponds to a wavelength of $\lambda \approx 400$m, while the upper bound $kL_u = 15$ corresponds to $\lambda \approx 134$m. Thus variation over typical ocean wavelengths is accounted for and the chosen values correspond to reasonable array lengths. The values are also chosen to allow comparison with previous literature, such as [9, 10], where similar values are chosen. It should be noted that the method is applicable for any reasonable values and, if desired, values can be chosen that correspond to a particular WEC array site if that information is available.

Strictly, the displacement amplitude δ_j is required to be positive by definition, so for a maximum displacement constraint of δ_{max}, the range of the displacement variables would be $0 \leq \delta_j \leq \delta_{max}$ and $0 \leq \psi_j \leq 2\pi$. However, mathematically this is equivalent to allowing the amplitude to be negative and restricting the phase to $0 \leq \psi_j \leq \pi$. Since the ψ_j variables are contained within a complex exponential expression, the variation over this variable within the optimisation would be more computationally intensive than variation over δ_j, albeit only slightly. However, given the large number of calls to the objective function and the large number of runs of the optimisation necessary, every effort was made to make the calculations more efficient. Therefore, in the implementation, a new variable χ_j is introduced and the displacements are written as

$$D_j = \chi_j e^{i\psi_j}. \tag{9}$$

If δ_{max} is a given amplitude constraint, then the limits on the displacement variables are $-\delta_{max} \leq \chi_j \leq \delta_{max}$ and $0 \leq \psi_j \leq \pi$ for $j = 1, \ldots, N$.

The optimisations are implemented in FORTRAN using a similar method to [10], where Numerical Analysis Group (NAG)[1] routine E04UCF[2] was employed to find the maximum of the objective function. This algorithm searches for the minimum value of the objective function using a sequential quadratic programming method. This algorithm is essentially identical to the subroutine NPSOL described in [12]. Appropriate NAG routines were also employed for the calculation of Bessel functions and quadrature. Motion

[1] http://www.nag.co.uk

[2] https://www.nag.co.uk/numeric/fl/manual/pdf/E04/e04ucf.pdf

constraints of $\delta_{max} = 2$ and $\delta_{max} = 3$ are examined.

The optimisation routine E04UCF requires a starting point to perform the optimisation. Therefore, in order to ensure a global optimum is found for a given problem, an exhaustive search of the space of starting points must be performed. For an array of five WECs, all possible combinations of $n_l \in \{0.1, 0.2, \ldots, 0.7\} \cup \psi_j \in \{0, \frac{\pi}{2}, \pi\} \cup \delta_j \in \{-3, -1, 1, 3\}$ for $l = 1, \ldots, 4$ and $j = 1, \ldots, 5$ are examined for $\delta \leq 3$. For the lower constraint $\delta \leq 2$, the set of starting points for WEC motion amplitude was taken to be $\delta_j \in \{-2, 0, 2\}$, with starting points for the other variables unchanged. It was found that the optimisation behaved quite well with respect to the starting values of δ_j and ψ_j, as the optimisation converged quickly and repeatedly to the same optimal solution, hence the relatively sparse sampling of starting points of these variables.

3. Constrained Optimisation Results

3.1. Comparison with Unconstrained Optimal Layout

The constrained performance of the optimal formation of an array of five devices in a linear geometry (previously identified in [10]) is now examined. With the optimal spacing denoted by $\mathbf{n}^*$, the array is subject to the direction of the incident waves. As the layout is prescribed prior to constrained optimisation, there are ten variables for $N = 5$ devices, namely the amplitudes δ_j and phases ψ_j of the displacements of each WEC. The objective function is given by (8) with $\mathbf{n} = \mathbf{n}^*$ fixed. This optimisation was performed for $\beta_0 = 0, \frac{\pi}{4}, \frac{\pi}{2}$.

Table 1 lists the optimal layouts $\mathbf{n}^*$ from the unconstrained optimisation

Table 1: Performance of optimal layouts from [10] subject to motion constraints

β_0	n_1^*	n_2^*	n_3^*	n_4^*	$I_{opt}(\delta \leq \infty)$	$\overline{I}_{opt}(\delta \leq 3)$	$\overline{I}_{opt}(\delta \leq 2)$
0	0.0500	0.0500	0.0500	0.8500	1.4802	0.5469	0.4691
$\frac{\pi}{4}$	0.0500	0.8500	0.0500	0.0500	1.1431	0.3070	0.2624
$\frac{\pi}{2}$	0.0500	0.2252	0.3859	0.3359	1.3643	0.9486	0.7693

in [10], along with the performance of these arrays in the unconstrained case (denoted by I_{opt}) and when a WEC motion constraint of $\delta \leq 2$ or $\delta \leq 3$ is enforced (denoted by $\overline{I}_{opt}$). The values of the displacement variables δ_j and ψ_j are listed in table 2. The computation time for each case examined in this section was of the order of ten minutes. This was due to the exhaustive search and optimisation routines scanning over ten variables.

As expected, performance is poorer when constraints are applied, with the lower constraint having a greater impact. For the $\beta_0 = 0, \frac{\pi}{4}$ cases, the application of constraints causes a reduction in performance of at least 63%, with only a relatively small difference between $\delta \leq 2$ and $\delta \leq 3$. This is most likely due to the presence of grouped devices in these layouts and the associated large motions for the unconstrained optimum. Since the optimal motions are predicted to be $\mathcal{O}(100) - \mathcal{O}(1000)$ from [10], it is anticipated that limiting the motions to $\mathcal{O}(1)$ would have a large effect on array performance. This also explains the relatively small difference between the two constraints, as the relative difference between $\delta = 2$ or 3 and $\delta = \mathcal{O}(100) - \mathcal{O}(1000)$ is also small.

The application of constraints seems to have a smaller impact on the $\beta_0 = \frac{\pi}{2}$ array. This is probably due to the larger spacing between most of the

Table 2: Optimal WEC displacement parameters for optimal layouts from [10] subject to constraints

β_0	δ_{max}	δ_1	δ_2	δ_3	δ_4	δ_5	ψ_1	ψ_2	ψ_3	ψ_4	ψ_5
0	2	-2.0000	-2.0000	2.0000	2.0000	-0.5326	0.8933	1.7679	0.0542	1.0235	2.5317
	3	-3.0000	-3.0000	-3.0000	3.0000	-0.5174	0.5977	1.8731	3.1236	1.3434	2.6386
$\frac{\pi}{4}$	2	-2.0000	-2.0000	-1.2500	2.0000	-1.4587	1.1384	2.6780	1.5186	0.8910	0.1221
	3	-3.0000	-3.0000	-1.6884	3.0000	-1.9200	0.8875	2.9290	1.3618	0.8832	0.3028
$\frac{\pi}{2}$	2	-2.0000	-1.1760	-2.0000	-2.0000	-2.0000	1.7266	1.7266	1.7266	1.7266	1.7266
	3	-3.0000	-0.1103	-3.0000	-3.0000	-3.0000	1.7266	1.7266	1.7266	1.7266	1.7266

devices in this layout and the smaller associated motions. The application of the $\delta \leq 3$ and $\delta \leq 2$ constraints results in performance losses of approximately 31% and 44% respectively. It does not appear to be possible for these fixed layouts to maintain average constructive interference ($\overline{I} > 1$) after the application of constraints, although moderate performance of $\overline{I} = 0.94859$, albeit slightly destructive, is achieved for $\beta_0 = \frac{\pi}{2}$ with $\delta \leq 3$.

Table 2 shows that, overall, the majority of the amplitude variables δ_j converged to the enforced limit of 2 or 3. It should be noted that all optimal arrays resulted in one or two of the δ_j values not converging to the limit but instead to some value in the centre of the allowed range. This indicates that within the constrained problem, the best solution does not result from simply setting all device amplitudes to their largest permissable values. The optimal constrained case appears to be when one or two WECs oscillate at a smaller amplitude with the appropriate choice of phase. This could be an artifact of forcing the WECs to be arranged in a layout which

was optimised for optimal unconstrained motions. In general, the phases of each WEC displacements are all different within each optimal solution found, with the obvious exception of the $\beta_0 = \frac{\pi}{2}$ array. For both constraints applied, all the WEC phases were equal in the optimal beam seas arrays.

A more detailed analysis of the constrained performance of these arrays is given in section 3.2, where the array layout is allowed to vary within a constrained optimisation. The performance of the array layouts previously identified as optimal in the unconstrained optimisation are then compared to the performance of the arrays where the WEC positions are not fixed and are also fed into the optimisation as variables.

3.2. Undetermined Layout

The performance of linear arrays is now optimised without a prescribed layout, so that the array formation and the device displacements are variables of the optimisation, giving a total of $3N-2 = 13$ variables for $N = 5$ WECs. This is performed for two different maximum displacement constraints of $\delta \leq 2, 3$ and the three values of prescribed incident wave angle $\beta_0 = 0, \frac{\pi}{4}, \frac{\pi}{2}$. The results of the optimisations are listed in table 3 and the optimal values of δ_j and ψ_j are listed in table 4. The optimal constrained layouts are denoted as $\mathbf{n}_{opt}$. In this section, the computation times for each case examined was of the order of one hour. The increase in computation time was due to the exhaustive search and optimisation routines scanning over 13 variables, three more variables than the optimisation in section 3.1.

As in the procedure employed in [10], minimum and maximum values of each separation parameter were enforced within the optimisation so that $0.05 \leq n_l \leq 0.85$ for $l = 1, \ldots, 4$. This ensures that no device will be

Table 3: Optimal linear array layout parameters subject to motion constraints

β_0	δ_{max}	$n_{opt,1}$	$n_{opt,2}$	$n_{opt,3}$	$n_{opt,4}$	$\overline{I}_{opt}$
0	2	0.0978	0.0532	0.1139	0.7351	0.49441
	3	0.1057	0.0504	0.1048	0.7391	0.58438
$\frac{\pi}{4}$	2	0.0940	0.1532	0.2259	0.5269	0.42508
	3	0.1310	0.3066	0.1103	0.4521	0.45507
$\frac{\pi}{2}$	2	0.2679	0.2321	0.2321	0.2679	0.87771
	3	0.2679	0.2321	0.2321	0.2679	1.06779

Table 4: Optimal WEC displacement parameters for constrained optimal layouts in table 3

β_0	δ_{max}	δ_1	δ_2	δ_3	δ_4	δ_5	ψ_1	ψ_2	ψ_3	ψ_4	ψ_5
0	2	-2.0000	-2.0000	2.0000	2.0000	-0.5044	0.9841	2.6244	0.3064	2.0858	2.5309
	3	-3.0000	-3.0000	3.0000	3.0000	-0.4828	0.7737	2.6660	0.3878	2.4455	2.5965
$\frac{\pi}{4}$	2	-2.0000	-2.0000	2.0000	1.5094	0.5083	1.1987	2.6658	0.5846	1.9964	2.0989
	3	-3.0000	3.0000	2.4695	-1.7879	0.5566	1.2333	0.1285	1.0368	0.2747	2.4616
$\frac{\pi}{2}$	2	-2.0000	-2.0000	-2.0000	-2.0000	-2.0000	1.7266	1.7266	1.7266	1.7266	1.7266
	3	-3.0000	-3.0000	-3.0000	-3.0000	-3.0000	1.7266	1.7266	1.7266	1.7266	1.7266

within 5% of the total array length of another device. The upper bound of 0.85 was chosen to allow the possibility that all but one of the separations was exactly the minimum bound. A 5% minimum constraint was chosen as this value also avoided possible difficulties due to numerical inaccuracies and poor behaviour of the objective function caused by small non-dimensional separation arguments. It is also a physically reasonable lower bound on WEC separation distances.

The unconstrained optimal layout $\mathbf{n}^*$ and the constrained optimal layouts $\mathbf{n}_{opt}$ are presented for each case of $\beta_0 = 0, \frac{\pi}{4}$ and $\frac{\pi}{2}$; the performance of the arrays are also analysed for variation in kL and β respectively. There are five curves in each $\overline{q}$ plot for each value of β_0 and these are intended to show the performance of the unconstrained optimal array $q(\mathbf{n}^*)$, the constrained arrays with the unconstrained optimal layout $\overline{q}(\mathbf{n}^*)$ for both $\delta \leq 2$ & $\delta \leq 3$ and the optimal constrained arrays with re-optimised layouts $\overline{q}(\mathbf{n}_{opt})$ for both $\delta \leq 2$ and $\delta \leq 3$.

It is anticipated that each constrained array would perform poorer that the unconstrained equivalent and it is also expected that

$$\overline{I}(\mathbf{n}_{opt}, \delta \leq 3) > \overline{I}(\mathbf{n}^*, \delta \leq 3) > \overline{I}(\mathbf{n}_{opt}, \delta \leq 2) > \overline{I}(\mathbf{n}^*, \delta \leq 2). \qquad (10)$$

However, it is unclear how sharp the inqualities will be, i.e how close to equality they can become. It is only by consideration of the individual cases that this information can be obtained.

Similar conclusions to the previous section can be drawn from table 4, where the majority of δ_j values converge to the limit of δ_{max} imposed. In head and intermediate seas, one or two δ_j did not converge to the maximum allowed value and all WECs have different phases ψ_j. However, in beam seas,

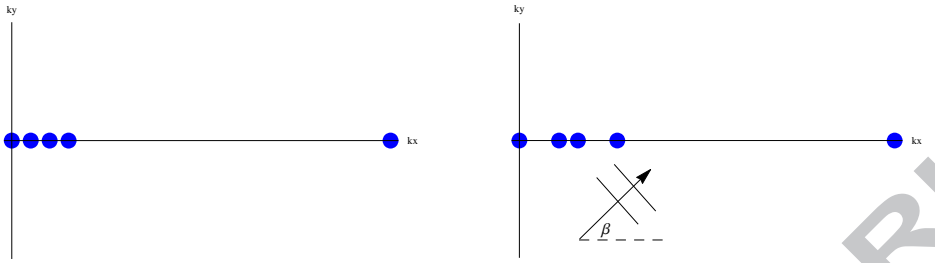

(a) Unconstrained (b) $\delta \leq 2, 3$

Figure 1: Constrained and unconstrained optimal linear arrays for $\beta_0 = 0$. The optimal layout for the $\delta \leq 3$ case is very similar to the $\delta \leq 2$ case and is omitted for clarity

$\delta_j = \delta_{max}$ and the phases are equal for all WECs, as would be expected. This is unlike the results in table 2, since in this case the WECs were optimised for constrained motions. Thus for beam seas, where the wave hits all WECs at the same time, the array is contrived such that the displacement limit is reached for all WECs, thereby maximising power capture.

3.2.1. Head Seas

Figure 1 shows the unconstrained and constrained optimal layouts for $\beta_0 = 0$. The constrained array layouts are quite similar for $\delta \leq 2$ and $\delta \leq 3$ and so the lower value is not shown. The unconstrained and constrained arrays all have four devices grouped to the left of the array, but, and perhaps surprisingly, these are more separated for the constrained layouts. Note that WECs 2 and 3 are still placed very close together, which may still cause some physical issues such as shadowing and possible collisions.

From figure 2, the overall behaviour of the constrained arrays is similar to the unconstrained array, in that there is small variation throughout $kL \in [5, 15]$. However, a considerable reduction in performance is caused by the

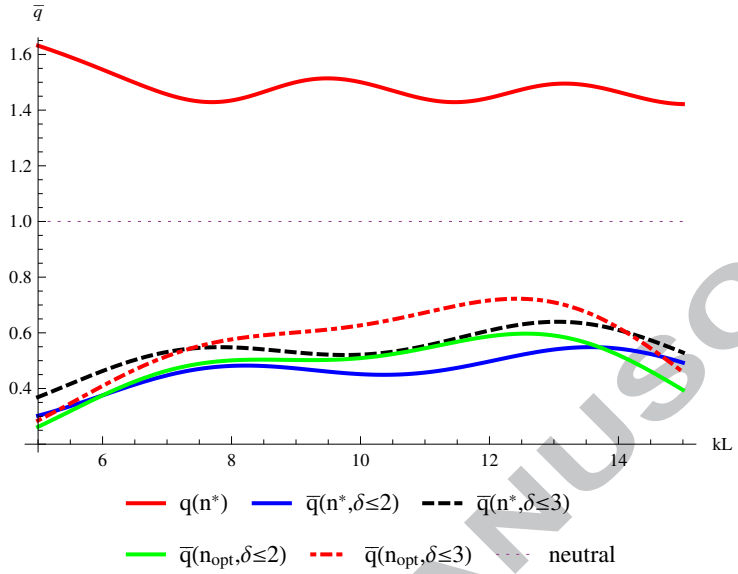

Figure 2: Performance of constrained and unconstrained linear arrays for variation in kL with $\beta = \beta_0 = 0$

application of constraints, as also indicated by utilisation and comparison of tables 1 and 3. Figure 3 shows that the constrained arrays have the advantage of a much broader peak performance in β-variation than the unconstrained array, although the peak is much lower. The unconstrained array has a range where $q > 1$ of approximately $\pm\frac{\pi}{8}$, while the constrained arrays have a larger range of $\pm\frac{\pi}{4}$ where $\overline{q} \approx 0.5$. This coupled with the low variation of $\overline{q}$ with kL suggests a large stability of performance for these constrained arrays in this case, although the performance achieved is rather poor in comparison to the same number of isolated devices. It should also be noted from figure 3 that the $\overline{q}$ values become negative outside a certain range, indicating that the constrained power absorbed by the array is negative in this case and the WECs are injecting power into the waves rather than absorbing power.

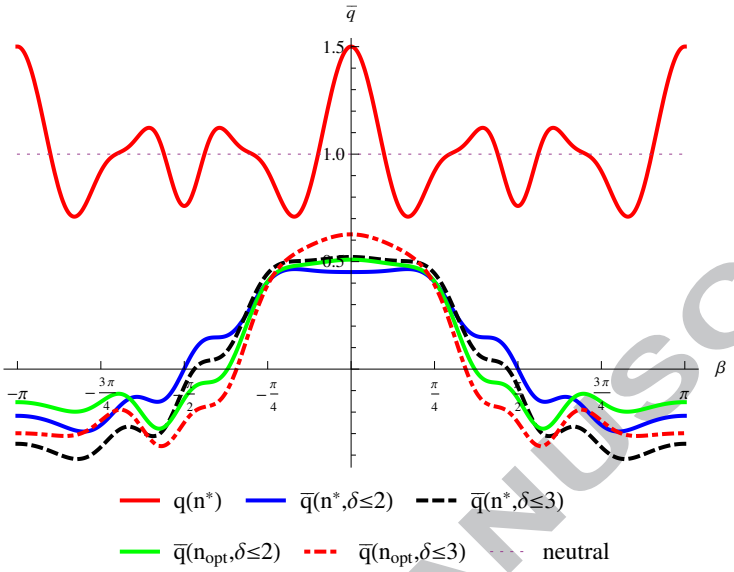

Figure 3: Performance of constrained and unconstrained linear arrays for variation in β with $\beta_0 = 0$ and $kL = 10$.

3.2.2. Intermediate Seas

Figure 4 shows the unconstrained and constrained optimal layouts for $\beta_0 = \frac{\pi}{4}$. As for head seas, the optimal constrained arrays are more separated in comparison to to the unconstrained optimal layout. However, in this case, the optimal layouts corresponding to $\delta \leq 2$ and $\delta \leq 3$ differ. In both constrained cases, WEC 5 is relatively isolated at the right of the array. For the $\delta \leq 2$ array, WECs 1-4 have an increasing separation between them, with the smallest separation between WECs 1 and 2 being 9.4% of the total length. In contrast, the $\delta \leq 3$ array has two pairs of devices approximately $0.11kL - 0.13kL$ apart, with the distance between the pairs being approximately $0.3kL$.

Figures 5 and 6 show the performance of the constrained arrays, along

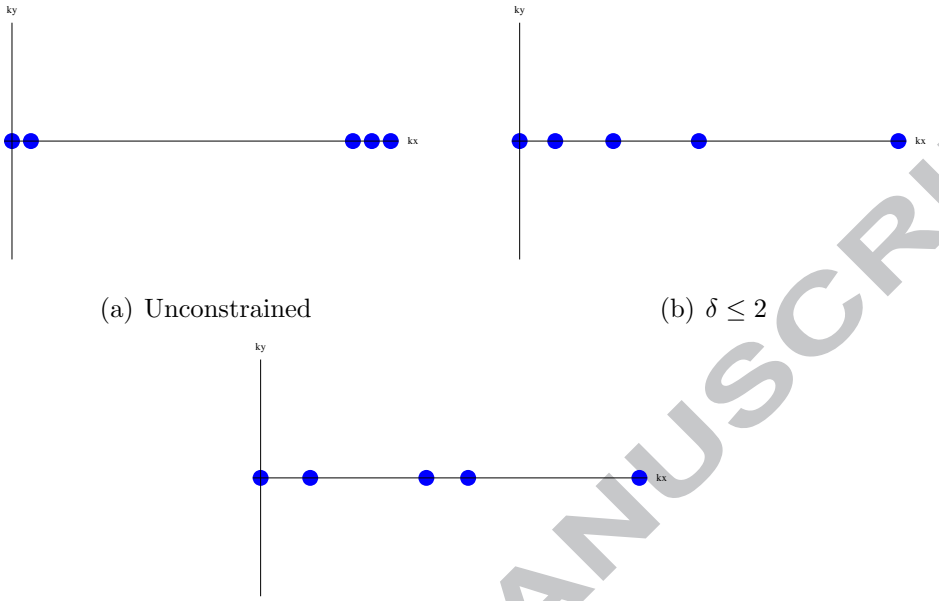

(a) Unconstrained

(b) $\delta \leq 2$

(c) $\delta \leq 3$

Figure 4: Constrained and Unconstrained Optimal linear arrays for $\beta_0 = \frac{\pi}{4}$.

with the unconstrained case, with kL and β variation respectively for $\beta_0 = \frac{\pi}{4}$. Similar to the head seas case, the application of amplitude constraints has a considerable influence on the array performance, with an overall reduction from $q \in [0.9, 1.3]$ to $\overline{q} \in [0.1, 0.6]$ for the kL variation. This is most likely due to the presence of closely spaced groups of WECs and associated large motions in the optimal unconstrained case.

The expected trend of $\delta \leq 3$ outperforming $\delta \leq 2$ is not evident in this case, as it is clear from figure 5 that $\overline{q}(\mathbf{n}_{opt}, \delta \leq 2) > \overline{q}(\mathbf{n}^*, \delta \leq 3)$. This is most likely because the optimal array layout is considerably different when constraints are applied. Therefore, applying constraints to the unconstrained

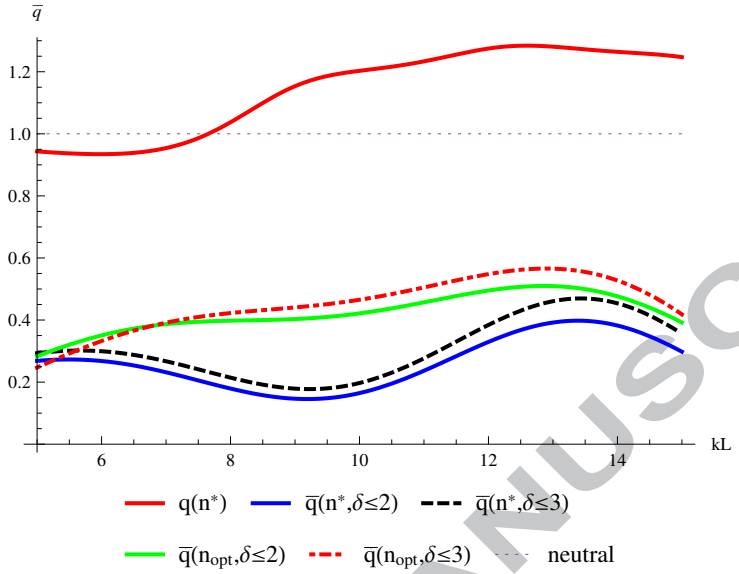

Figure 5: Performance of constrained and unconstrained linear arrays for variation in kL with $\beta = \beta_0 = \frac{\pi}{4}$

optimal layout results in very poor performance. This figure also shows that

$$\overline{I}(\mathbf{n}_{opt}, \delta \leq 3) > \overline{I}(\mathbf{n}_{opt}, \delta \leq 2) > \overline{I}(\mathbf{n}^*, \delta \leq 3) > \overline{I}(\mathbf{n}^*, \delta \leq 2), \qquad (11)$$

in contrast with expectation (10) and the results in head seas.

As with head seas, the constrained array performance varies relatively slowly with kL. This indicates that the performance of the array is relatively stable to changes in kL, although a large reduction in interaction factor is again seen when constraints are imposed. Examination of figure 6 shows a similar behaviour to head seas, where a broader performance with respect to β is achieved around $\beta = 0$. This is not beneficial in this case, as the target wave angle is $\beta_0 = \frac{\pi}{4}$, around which are significant variations in $\overline{q}$. This is particularly evident for $|\beta| > \frac{\pi}{4}$, where the $\mathbf{n}_{opt}$ arrays give $\overline{q} < 0$

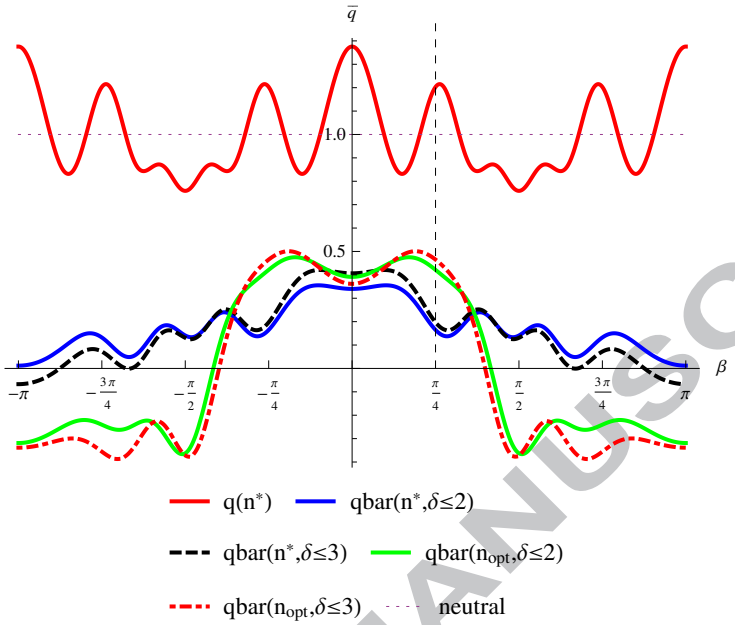

Figure 6: Performance of constrained and unconstrained linear arrays for variation in β with $\beta_0 = \frac{\pi}{4}$ and $kL = 10$. The target wave angle $\beta_0 = \frac{\pi}{4}$ is shown by the vertical dashed line.

for $|\beta| > \frac{3\pi}{8}$. The $\mathbf{n}^*$ arrays are slightly more stable around the target wave angle, although the performance is not as high as the $\mathbf{n}_{opt}$ arrays.

3.2.3. Beam Seas

Figure 7 shows the optimal constrained and unconstrained array layouts for beam seas. The optimal layout in both constrained cases is very close to a uniform array. This reinforces the intuitive idea that constrained arrays tend to have their optimal layouts more spaced apart, avoiding groups of WECs, with the exception of the head seas. It is also consistent with the idea that greater frontage to the waves gives greater power absorption, since an array with greater frontage to the incident wave has a greater amount of

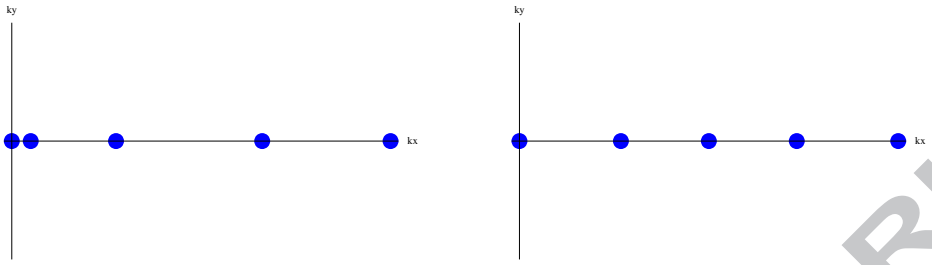

(a) Unconstrained (b) $\delta \leq 2, 3$

Figure 7: Constrained and Unconstrained Optimal linear arrays for $\beta_0 = \frac{\pi}{2}$. The optimal layout for $\delta \leq 3$ is identical to the $\delta \leq 2$ case

wave-power incident upon it. However, as shown in previous studies, this does not always translate into increased power absorption of better WEC interference. The $\overline{I} > 1$ property is achieved for the $\delta \leq 3$ constraint at this wave angle; this is the only case where average constructive interference is maintained after the application of constraints.

The performance of the arrays for beam seas are shown in figures 8 and 9 for variation in kL and β respectively. Both figures show that the application of constraints does not have as severe a negative impact on $\overline{q}$ in comparison with other wave angles. A loss is seen for the $\overline{q}$ values in compared to q, but constructive interference is still achieved in some cases. As with the $\beta_0 = 0$ case, a constraint of $\delta \leq 2$ has a greater impact on performance than $\delta \leq 3$; within this pattern, the $\mathbf{n}_{opt}$ arrays perform better than the $\mathbf{n}^*$ layouts, so that (10) holds true, as expected.

As in the previous two configurations, figure 8 shows the slow variation of $\overline{q}$ with kL, indicating that a small change in kL produces only a small change in array performance. In general, this figure shows that better performance is achieved for larger values of kL within the domain examined. Constructive

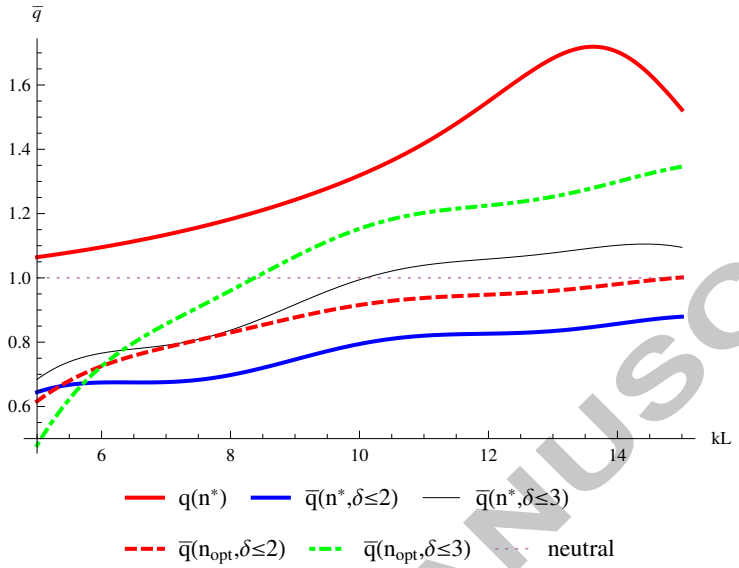

Figure 8: Performance of constrained and unconstrained linear arrays for variation in kL with $\beta = \beta_0 = \frac{\pi}{2}$

interference $\overline{q} > 1$ is achieved for the $\delta \leq 3$ arrays, while the best case for $\delta \leq 2$ is $\overline{q} \approx 1$ at $kL = 15$ for the $\mathbf{n}_{opt}$ layout. Both configurations with $\delta \leq 2$ resulted in $\overline{q} \leq 1$. The fact that $\overline{q}(\mathbf{n}_{opt}, \delta \leq 3) \approx 1.2$ for $kL \in [10, 15]$ is promising, as this indicates that constructive interference is still possible after the imposition of a reasonable constraint. This layout is also almost uniformly-spaced and so avoids the difficulties associated with closely spaced devices.

The β-variation of the array performances are shown in figure 9. Contrary to head and intermediate seas, the imposition of constraints result in a narrower peak performance around $\beta = \beta_0 = \frac{\pi}{2}$ compared to the unconstrained case. A high peak value is achieved with $\max[\overline{q}] \in [0.8, 1.2]$ depending on the constraint and layout but the peak is significantly narrower. This results in

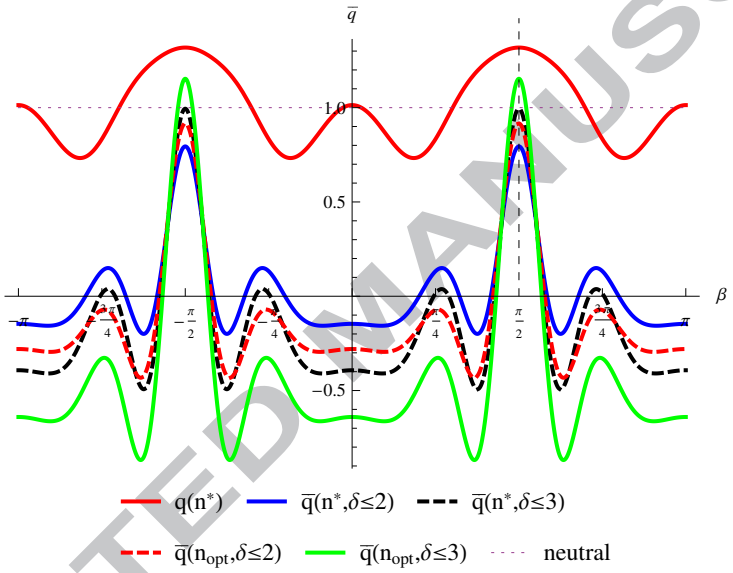

Figure 9: Performance of constrained and unconstrained linear arrays for variation in β with $\beta_0 = \frac{\pi}{2}$ and $kL = 10$. The target incident wave angle $\beta_0 = \frac{\pi}{2}$ is shown by the vertical dashed line.

$\overline{q} < 0$ for a relatively small change of $\beta_0 \pm \frac{\pi}{12}$, which may be undesirable and is highly dependent upon the angular variation within the incident wavefield.

The results of figure 8 can be compared with the work on constrained motion performance of the uniform array in [3] (figure 6). In both cases, the constrained array examined is almost identical in geometry, since the constrained array presented here ($\mathbf{n}_{opt}$) for beam seas is almost uniform. Note in [3] that the quantity examined is the absorption length scaled by the total WEC covering in the array $\frac{l_{abs}}{10a}$. Note also that this quantity is assessed with respect to variation in the device spacing kd, not the array length kL. Agreement is seen, however, in the overall performance of the array with respect to the application of constraints, i.e. an application of a constraint of three time the wave amplitude still allows for constructive interference, while a constraint of twice the wave amplitude is severely limiting and results in destructive interference dominating.

4. Discussion and Conclusion

This paper extends the work of [9] and [10] to linear arrays where the WECs are constrained to oscillate at no more than two or three times the incident wave amplitude. This is necessary as nearly all unconstrained optimal arrays in these works resulted in predicted optimal displacement amplitudes well in excess of the incident wave amplitude. Such large displacements would not only cause significant physical and engineering difficulties but also violate the underlying linear wave theory, which assumes WEC motions are at most the same order of magnitude as the wave motions and are assumed small in some sense. Therefore, an investigation of placing constraints on

WEC motions is necessary to add validity to the results and conclusions of previous studies in unconstrained regimes.

It should be noted that all models of the type implemented within this work inherently overestimate the the actual power absorption of a WEC. This model considers the hydrodynamic power absorbed by the device, so a PTO is not directly implemented within this work. If a PTO term was included in the equation of motion and the power absorbed calculated from this term alone, then this term would absorb a fraction of the total hydrodynamic power. However, this would result in more intensive calculations and impede a numerical optimisation of the type performed in this preliminary work.

The imposition of constraints has been shown to have a significant impact on array performance, particularly when optimal performance was accompanied by by very large device motions. In previous studies, the impression of good performance was given by the large values of optimal interaction factor q achieved. However, these were accompanied in most cases by unacceptably large device motions. Therefore, the application of constraints was expected to have a large negative impact on array performance. This was particulary true in those cases with groups of closely spaced devices, which were associated with the largest predicted optimal motions.

This effect is most clearly seen by comparing the results of head seas and beam seas in figures 1 and 7. The $\beta_0 = 0$ unconstrained optimal layout from [10] contained a group of four devices and predicted very unrealistic motions of the order of 1000 times the wave amplitude. When constraints are applied, the array performance is reduced by approximately 60% and

resulted in the domination of destructive interference ($\overline{q} < 1$). In contrast, the $\beta_0 = \frac{\pi}{2}$ unconstrained optimal array was more spaced, although still contained a closely spaced pair of WECs. The application of constraints here resulted in a smaller performance reduction of approximately 30% (for $\delta \leq 3$) and allowed the possibility of constructive interference ($\overline{q} > 1$).

When the array layout parameters were added as optimisation variables, noticeably different layouts were obtained in comparison to the unconstrained optimisation (i.e. $\mathbf{n}^* \neq \mathbf{n}_{opt}$). This resulted in a more separated layout in each case, which reduced the number closely-spaced WECs within the array or eliminated these groups of WECs altogether. For $\beta_0 = 0$, the constrained optimal layout separated the group of four devices slightly but still retained a closely spaced pair. This was very similar for both $\delta \leq 2$ and $\delta \leq 3$. In the intermediate case of $\beta_0 = \frac{\pi}{4}$, no closely spaced devices remained in the constrained optimal layouts. Most notably, the different constraints resulted in significantly different optimal layouts for this wave angle. A symmetric and almost uniform layout was found to be optimal when the constraints were applied in the beam seas case, with the same layout found for both $\delta \leq 2$ and $\delta \leq 3$. This optimisation eliminated the pair of closely spaced devices on the left of the unconstrained optimal layout for this wave angle. This was also the best performing constrained array with the largest $\overline{I}$ for both constraints, with mean constructive interference ($\overline{I} > 1$) maintained for the $\delta \leq 3$ constraint. The fact that the optimal array layout changes with the constraint imposed agrees with the result of [13], which shows that the control problem is related to the array layout problem.

Although both constraints considered were within the $\mathcal{O}(1)$ regime nec-

essary, the $\delta \leq 2$ constraint had a more severe impact on array performance; this was not unexpected. In general, the arrays with the $\delta \leq 3$ constraint applied performed better than the $\delta \leq 2$ arrays, with varying differences between these depending on the wave angle and layout considered. Previous studies, such as [3] and [6], have discussed how the imposition of a constraint of three times the wave amplitude still allows for constructive interference in some cases, while a constraint of two times the wave amplitude is severely restrictive. This idea is echoed here, where $\delta \leq 2$ had a greater negative impact on all arrays considered, while constructive interference was still possible in some cases for $\delta \leq 3$.

It would be reasonable to argue that the best linear array presented herein was the almost uniform layout found for $\beta_0 = \frac{\pi}{2}$. This array had the greatest overall performance with constraints imposed, by a considerable margin. The array was widely spaced and symmetric and thus avoided issues of closely spaced WECs. Most importantly, mean constructive interference was possible for the larger constraint and stable performance with respect to changes in kL was also observed. However, the array was very sensitive to changes in incident wave angle. Moving away from the target wave angle by $\pm\frac{\pi}{12}$ resulted not only in destructive interference, but also $\overline{q} < 0$, indicating that the array is adding power to the waves rather than extracting it.

It is often envisaged that WECs should be placed in large arrays or small arrays. In principle, the method presented in this paper can be applied to larger arrays of more than five WECs. However, the main issue with this is the increase in optimisation variables and the associated increase in computation time; this phenomenon is sometimes called "parameter explosion".

The optimisation must scan over the possible starting point space of all variables, and this scan must be fine enough to ensure that the global optimum is reliably and repeatedly found. The computation times become prohibitive for arrays of larger numbers of WECs. For example, an array of ten WECs would have twenty displacement variables and eight position variables, giving a total of 28 variables for a constrained layout optimisation. It is estimated that in order to conduct a sufficient scan of the starting point space in this case, the optimisation would take of the order of 50-100 hours on one standard machine. Thus the present study is limited to arrays of five WECs, as this also allows comparison with previous research such as [3, 6, 8, 9, 10].

The results presented here show that a trade-off is made either in overall performance of the array or in the sensitivity of the optimal array. When examining the β plot for the head seas case in figure 3, it is clear that the imposition of constraints widens the peak performance of the $\overline{q}$ vs β curve compared to the unconstrained case, although the overall performance is severely reduced. However, the opposite is seen for beam seas in figure 9, where decent performance is maintained under the imposition of constraints but the peak performance is significantly narrowed, thus severely increasing the sensitivity of the array to changes in the incident wave angle. Within the current analysis, it does not seem to be possible to have an array under motion constraints that both performs well and is stable to parameter changes.

Future work should include a more detailed investigation of this trade-off. One possible method to combat this issue would be to consider the objective function as the mean performance over the incident wave angle, rather than

a non-dimensional length. This is motivated by the greater effect that β has on the optimal array formation in comparison to changes in kL. This formation of the objective function would also allow for a generalised 2-D array layout optimisation, since no array geometry need be imposed. This will be considered in part 2 of this paper.

Acknowledgments

PhD funding for Justin P.L. McGuinness was provided by the Irish Research Council via a Government of Ireland Postgraduate Scholarship (GOIPG/2013/1197), and is gratefully acknowledged.

[1] D. V. Evans, Some theoretical aspects of three-dimensional wave-energy absorbers, in: Symposium on Ocean Wave Energy Utilization, 1979.

[2] J. Falnes, Radiation impedance matrix and optimum power absorption for interacting oscillators in surface waves, Applied Ocean Research 2 (2) (1980) 75–80.

[3] G. P. Thomas, D. V. Evans, Arrays of three-dimensional wave-energy absorbers, Journal of Fluid Mechanics 108 (1981) 67–88.

[4] P. McIver, Some hydrodynamic aspects of arrays of wave-energy devices, Applied Ocean Research 16 (2) (1994) 61–69.

[5] S. A. Mavrakos, P. McIver, Comparison of methods for computing hydrodynamic characteristics of arrays of wave power devices, Applied Ocean Research 19 (5-6) (1997) 283–291.

[6] C. Fitzgerald, Optimal configurations of arrays of wave power devices, Master's thesis, University College Cork (2006).

[7] C. Fitzgerald, G. P. Thomas, A preliminary study on the optimal formation of an array of wave power devices, in: European Wave and Tidal Energy Conferance, 2007.

[8] B. F. M. Child, On the configuration of arrays of floating wave energy converters, Phd thesis, The University of Edinburgh (2011).

[9] J. P. L. McGuinness, G. Thomas, Optimal arrangements of elementary arrays of wave-power devices, in: European Wave and Tidal Energy Conference, 2015.

[10] J. P. L. McGuinness, G. Thomas, Hydrodynamic optimisation of small arrays of heaving point absorbers, Journal of Ocean Engineering and Marine Energy 2 (4) (2016) 439–457.

[11] T. H. Havelock, Waves due to a floating sphere making periodic heaving oscillations, Proceedings of the Royal Society of London. Series A. Mathematical and Physical Sciences 231 (1184) (1955) 1–7.

[12] P. E. Gill, W. Murray, M. A. Saunders, M. H. Wright, User's guide for npsol (version 4.0): A fortran package for nonlinear programming., Tech. rep., DTIC Document (1986).

[13] P. B. Garcia-Rosa, G. Bacelli, J. V. Ringwood, Control-informed optimal array layout for wave farms, IEEE Transactions on Sustainable Energy 6 (2) (2015) 575–582.

- The constrained optimisation of linear arrays of heaving point absorber WECs is considered.

- Previous research is extended by constraining the WEC motion amplitudes to two or three times the incident wave amplitude.

- The objective function of the optimisation is taken to be the mean performance of the array, with respect to isolated devices, over a range of non-dimensional array length. This is defined using the averaged interaction factor.

- The results of the constrained optimisation are compared with previous results in an unconstrained regime.

- It found that the optimal constrained layouts are more separated than the unconstrained cases. Most notably, an almost uniform layout is found to be optimal for beam seas.